

Precise hypocenter distribution in and around the subducting seamount, Mw7.9 thrust event, and shallow tectonic tremor at the off-Ibaraki region, the southern part of northeast Japan

Shinji Yoneshima¹, Kimihiro Mochizuki¹, Tomoaki Yamada¹, and Masanao Shinohara¹

¹Earthquake Research Institute, University of Tokyo.

Contents of this file

Figures S1 to S9.

Introduction

This supporting information provides a supplemental description of the basic ocean bottom seismometer (OBS) experiment information and quality control of the event location processing result. Figure S1 presents the OBS experiment period for each OBS. Figure S2 depicts the V_p/V_s ratio of the sediment layer estimated from the PS-converted wave. Figure S3 presents a waveform example of a local event. Figure S4 presents Magnitude plots between the JMA magnitude and the OBS magnitude. Figure S5 shows the M-T diagram to present the lower limit's temporal change of the event magnitude detection. Figure S6 is the histogram of the error bar for the located events. Figure S7 presents the hypocenters from Shinohara et al. (2011, 2012). Figures S8 and S9 present the cross section of the error ellipsoid along with the seismic survey line of Line EW (Mochizuki et al. 2008) and Line 13 (Tsuru et al., 2002).

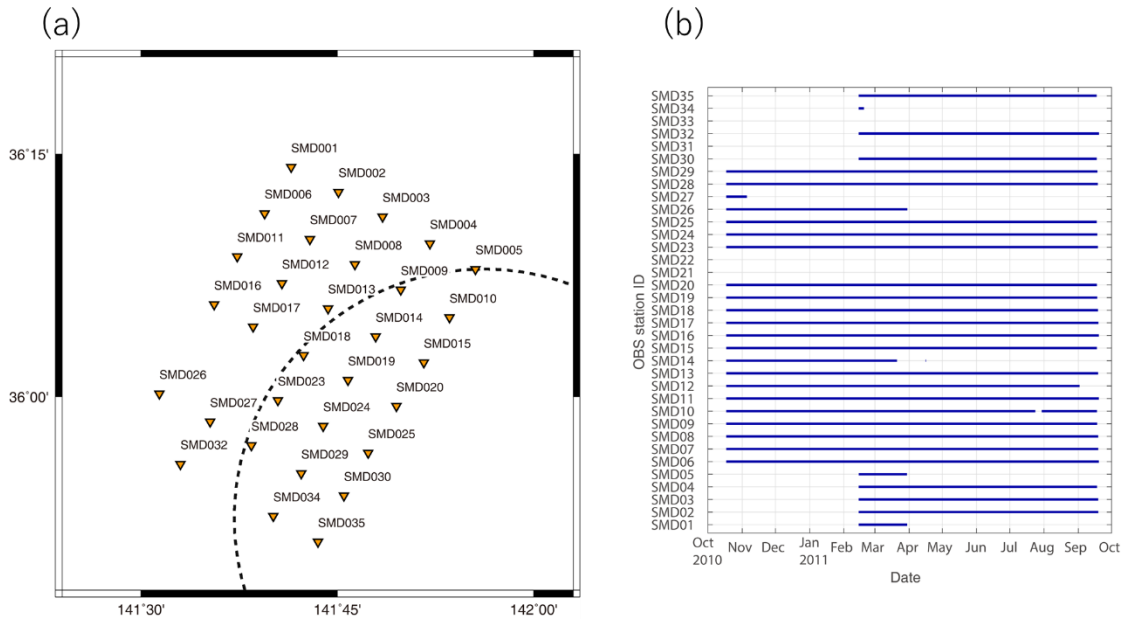


Figure S1. Label names of OBSs and observation period. (a) Plan map view with station labels. (b) Observation period of each OBS.

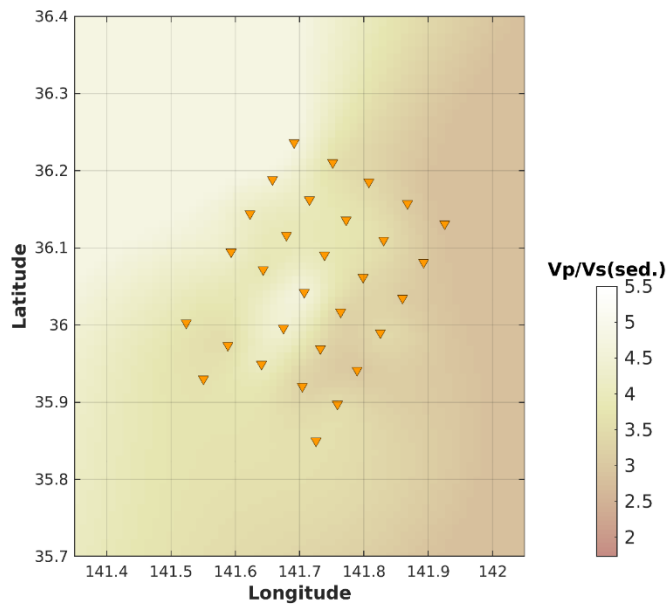


Figure S2. Estimated V_p/V_s ratio distribution in the sediment layer. The spatial interpolation that preserves an exact value just below the OBS site was applied (Smith & Wessel, 1990).

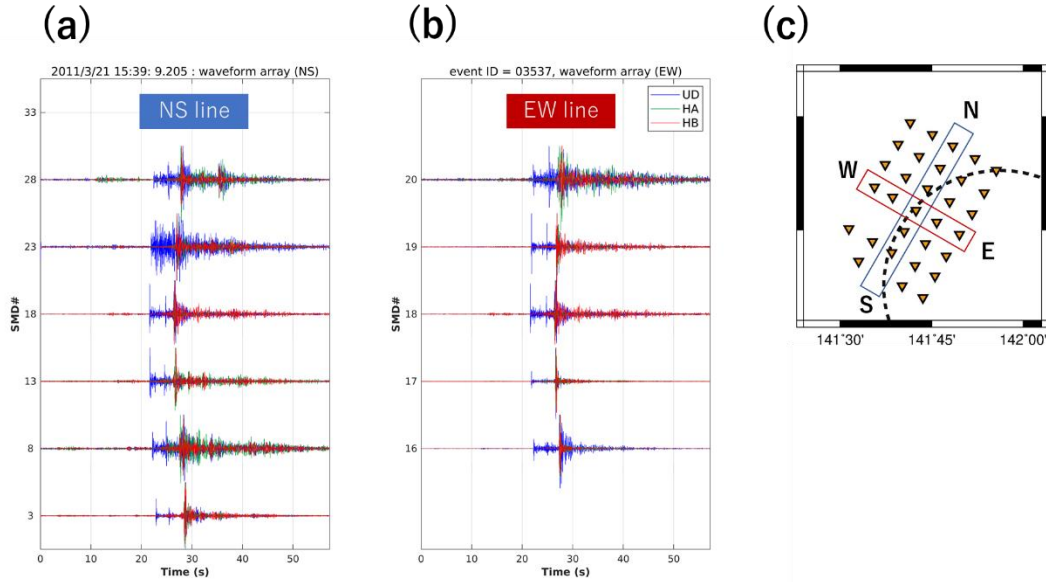


Figure S3. Example of the waveform recorded by OBSs. Each component of the waveform traces is normalized by the maximum amplitude. (a) North-south (NS) OBS arrays. Three-component waveforms are presented. (b) East-west (EW) OBS arrays. (c) Plan view of the OBS network showing the NS and EW arrays.

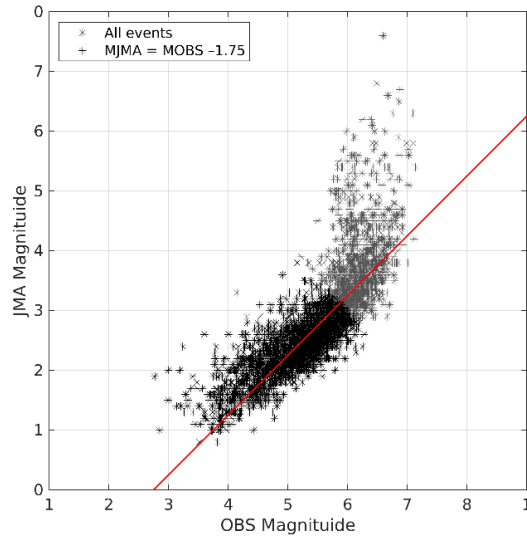


Figure S4. Uncorrected OBS magnitude versus JMA magnitude. The red line denotes the correction function after a line fit. The gray stars represent all the available events. The number of samples (N) is 3448. The black stars are the selected events for the fitting (N = 2467).

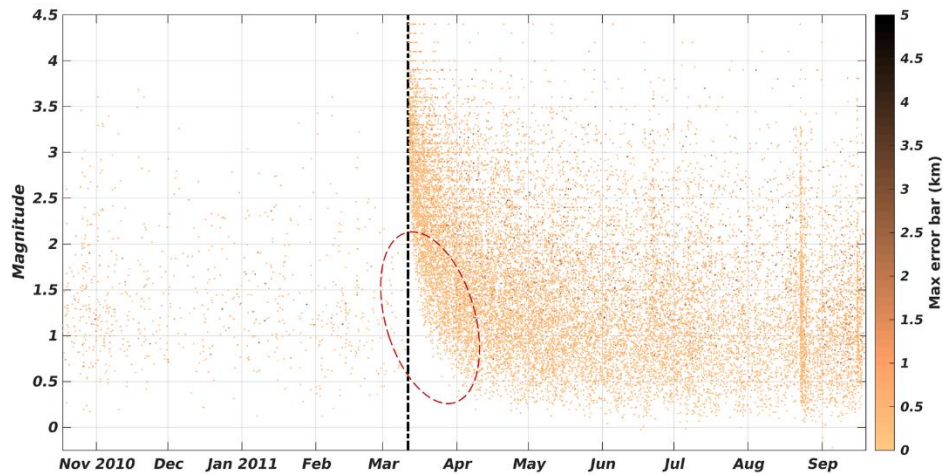


Figure S5. M-T diagram. The color of each dot denotes the error bar of the event. The vertical dot-dashed line presents the origin time of the 2011 Tohoku-oki earthquake. The red dashed circle presents the region of the degraded event detection performance.

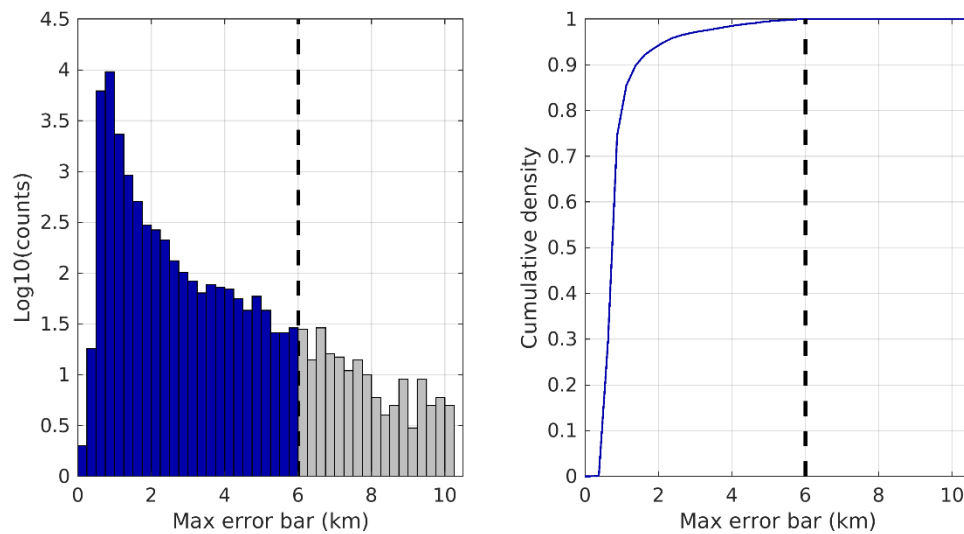


Figure S6. Error bar distribution. (Left) Histogram of the error bar with 95% confidence interval. Gray and dark blue bars are the error bars of the selected events within ± 6 km error bar, and all the events before the selection, respectively. The number of events before and after the selection are 22,562 and 21,242, respectively. The vertical dashed bar is the criteria of the event selection. (Right) Cumulative summation of the histogram.

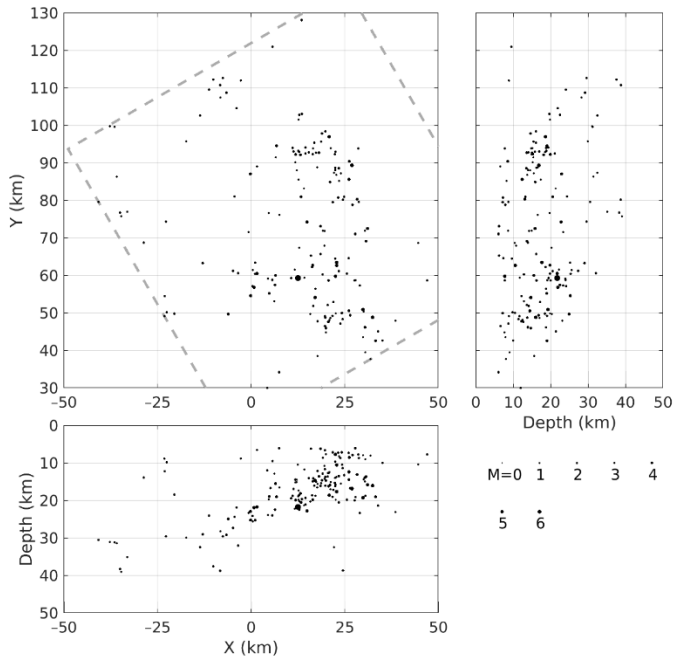


Figure S7. Cross-sectional view of the hypocenters (after Shinohara et al. 2011, 2012). The gray dashed rectangular area shows the study area used in this study.

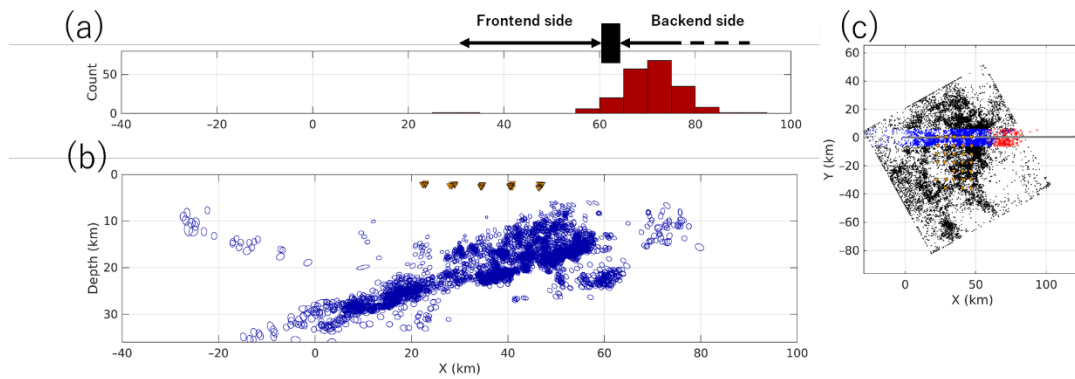


Figure S8. Error ellipsoids of events presented in Figure 10. (a) Same plot with Figure 10a. (b) Error ellipsoids of 68 % confidence interval for events shown in Figure 10b. (c) Same plot with Figure 10c.

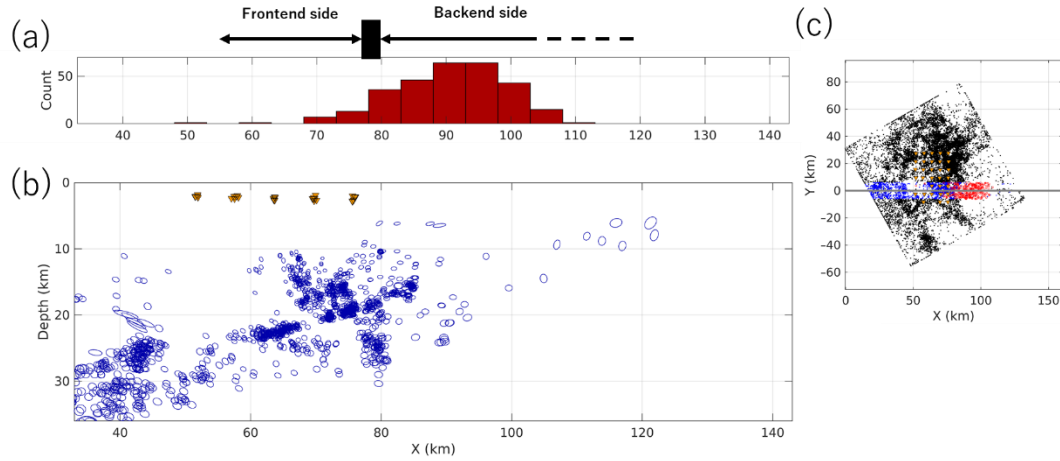


Figure S9. Error ellipsoids of events in presented Figure 11. (a) Same plot with Figure 11a. (b) Error ellipsoids of 68 % confidence interval for the events shown in Figure 11b. (c) Same plot with Figure 11c.